

# Strong Axiality and Ising Exchange Interaction Suppress Zero-Field Tunneling of Magnetization of an Asymmetric Dy<sub>2</sub> Single-Molecule Magnet

Yun-Nan Guo,<sup>†,‡</sup> Gong-Feng Xu,<sup>†</sup> Wolfgang Wernsdorfer,<sup>§</sup> Liviu Ungur,<sup>#</sup> Yang Guo,<sup>†</sup> Jinkui Tang,<sup>\*,†</sup> Hong-Jie Zhang,<sup>\*,†</sup> Liviu F. Chibotaru,<sup>\*,#</sup> and Annie K. Powell<sup>⊥</sup>

<sup>†</sup>State Key Laboratory of Rare Earth Resource Utilization, Changchun Institute of Applied Chemistry, Chinese Academy of Sciences, Changchun 130022, P. R. China

<sup>‡</sup>Graduate School of the Chinese Academy of Sciences, Beijing 100039, P. R. China

<sup>§</sup>Institut Néel, CNRS and Université J. Fourier, BP 166, 25 Avenue des Martyrs, 38042 Grenoble, France

<sup>#</sup>Division of Quantum and Physical Chemistry, Department of Chemistry, Katholieke Universiteit Leuven, Celestijnenlaan 200F, 3001 Leuven, Belgium

<sup>⊥</sup>Institute of Inorganic Chemistry, Karlsruhe Institute of Technology, Engesserstrasse 15, 76131 Karlsruhe, Germany

**S** Supporting Information

**ABSTRACT:** The high axiality and Ising exchange interaction efficiently suppress quantum tunneling of magnetization of an asymmetric dinuclear Dy<sup>III</sup> complex, as revealed by combined experimental and theoretical investigations. Two distinct regimes of blockage of magnetization, one originating from the blockage at individual Dy sites and the other due to the exchange interaction between the sites, are separated for the first time. The latter contribution is found to be crucial, allowing an increase of the relaxation time by 3 orders of magnitude.

The discovery of single-molecule magnet (SMM) behavior, where relaxation and quantum tunneling of the magnetization result from a molecular-based blocking anisotropy, is recognized as an important breakthrough in the field of molecular-based magnetism, with the promise of a revolution in data storage and processing.<sup>1</sup> Recent advances have shown the viability of lanthanide-based complexes in generating large barriers to spin reversal as a result of their significant magnetic anisotropy arising from the large, unquenched orbital angular momentum.<sup>2</sup> Indeed, a single anisotropic magnetic lanthanide ion in an axial crystal-field environment can provide conditions sufficient to establish a thermal barrier for reversal of the magnetization.<sup>3</sup> In the course of this recent research activity, the anisotropic barrier records have toppled like dominoes for lanthanide SMMs.<sup>4</sup> Such compounds advance the prospects of SMMs, bringing the goals of molecule-based information storage and processing closer to reality.<sup>5</sup>

However, there is an intrinsic drawback in that there are only very weak exchange interactions between the lanthanide ions as a result of the efficient shielding of the unpaired electrons in their 4f orbitals. The relaxation of magnetization in polynuclear clusters appears to arise largely from single ion anisotropy,<sup>6</sup> which is fundamentally different from the giant spin model, in

which the coupled system operates as a single magnetic unit.<sup>1a</sup> The hyperfine couplings and dipolar spin–spin interactions in lanthanide ions allow fast quantum tunneling of magnetization (QTM)<sup>7</sup> that prevents the isolation of zero-field lanthanide SMMs with large barriers.<sup>4b</sup> As a way to address this challenge, Long and colleagues successfully constructed strong magnetically coupled Dy<sup>III</sup> complexes through a N<sub>2</sub><sup>3−</sup> radical bridge, giving rise to a new record SMM.<sup>8</sup> This breakthrough demonstrates that a joint contribution, combining strong magnetic coupling with single-ion anisotropy, may ultimately lead to higher relaxation barrier SMMs capable of retaining their magnetization at more practical temperatures.<sup>8</sup>

In the present work, we describe a unique asymmetric dinuclear Dy<sup>III</sup> SMM, [Dy<sub>2</sub>ovph<sub>2</sub>Cl<sub>2</sub>(MeOH)<sub>3</sub>]·MeCN (**1**, where H<sub>2</sub>ovph = pyridine-2-carboxylic acid [(2-hydroxy-3-methoxyphenyl)methylene] hydrazide), in which the metal ions are ferromagnetically coupled. This compound provides a unique opportunity to probe simultaneously the contributions of both the exchange interaction and single-ion anisotropy to the relaxation dynamics of polynuclear lanthanide systems. Detailed magnetization dynamics studies reveal almost complete blockage of magnetization in this compound, which is further corroborated by *ab initio* calculations, indicating that the quantum tunneling pathways are strongly suppressed in low-lying exchange multiplets at low temperatures. In the high-temperature regime, the blockage of magnetization occurs at individual Dy sites, and two closely spaced relaxation processes operating via the excited Kramers doublets of individual Dy ions can be nicely resolved by the sum of two modified Debye functions.

The reaction of DyCl<sub>3</sub>·6H<sub>2</sub>O with H<sub>2</sub>ovph in 2:1 methanol/acetonitrile, in the presence of NaHCO<sub>3</sub>, produces yellow crystals of **1**, for which the asymmetric dinuclear unit, as determined by single-crystal X-ray diffraction, is depicted in Figure 1. The metal centers in the dinuclear core are bridged by the alkoxido groups (O1 and O4) of two antiparallel, or “head-to-tail” ovph<sup>2−</sup> ligands

Received: June 7, 2011

Published: July 11, 2011

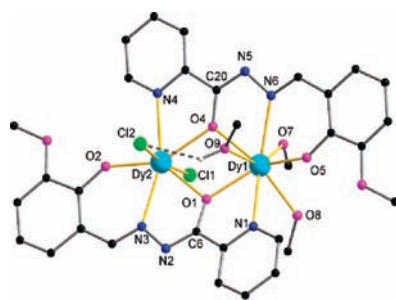


Figure 1. Asymmetric dinuclear unit of **1**.

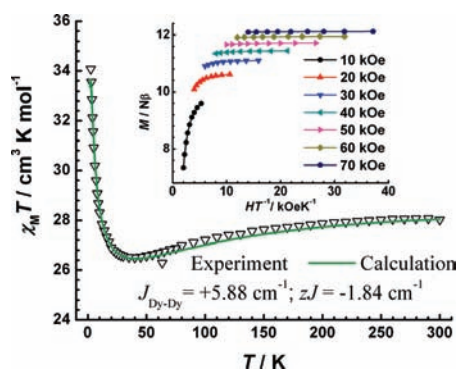


Figure 2. Plot of  $\chi_M T$  vs  $T$  for **1**. The solid line corresponds to the best fit. The inset is a plot of the reduced magnetization  $M$  vs  $H/T$ . The solid lines are guides for the eye.

(Scheme S1 in the Supporting Information (SI)), with the Dy···Dy distance being 3.8644 (5) Å and the two Dy–O–Dy angles 112.3(2) and 111.5(2)°. The pyridyl nitrogens (N1 and N4), the hydrazide nitrogens (N3 and N6), and the phenolate oxygens (O2 and O5) of the ligands also coordinate to the dysprosium centers. The coordination spheres of Dy1 and Dy2 are completed by three methanol molecules and two chloride ions, respectively. The eight-coordinate Dy1 center exhibits what has been described as a hula hoop-like geometry, where the cyclic ring (hula hoop) is defined by the atoms N1, O1, O4, N6, and O5.<sup>9</sup> The seven-coordinate Dy2 center has a nearly perfect pentagonal bipyramidal coordination environment (Figure S1). Strong intra- and intermolecular hydrogen-bonding interactions result in a one-dimensional supramolecular chain with an antiparallel arrangement of the molecules (Figure S2). The shortest intermolecular Dy···Dy distance is 7.5071(5) Å, which does not necessarily preclude any intermolecular exchange interactions.

Direct current (dc) magnetic susceptibility studies of a polycrystalline sample (Figure 2) reveal a room-temperature  $\chi_M T$  value of 28.1 cm<sup>3</sup> K mol<sup>-1</sup>, which is in good agreement with the expected value of 28.34 cm<sup>3</sup> K mol<sup>-1</sup> for two uncoupled Dy<sup>III</sup> ions (<sup>6</sup>H<sub>15/2</sub>,  $g = 4/3$ ). The  $\chi_M T$  product gradually decreases with lowering temperature, reaching a minimum value of 26.5 cm<sup>3</sup> K mol<sup>-1</sup> at about 40 K, which is mainly ascribed to the progressive depopulation of excited Stark sublevels.<sup>10</sup> The  $\chi_M T$  value then increases sharply to a maximum of 34.1 cm<sup>3</sup> K mol<sup>-1</sup> at 2.5 K, which obviously suggests the presence of intramolecular ferromagnetic interactions between the metal centers, as observed in other dysprosium compounds.<sup>4a,11</sup> The lack of a superposition of the  $M$  vs  $H/T$  data on a single master curve and the low

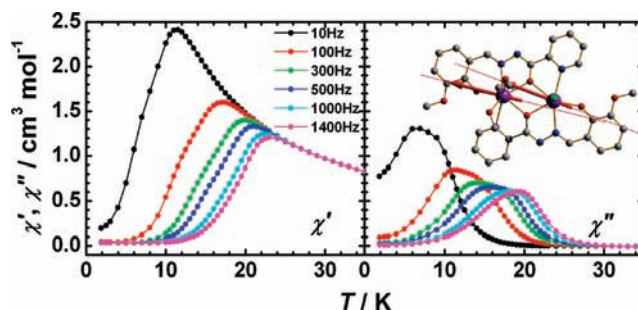


Figure 3. Temperature dependence of the in-phase ( $\chi'$ ) and out-of-phase ( $\chi''$ ) parts of the ac susceptibility for **1** under zero-dc field. The solid lines are guides for the eye. Inset: Orientations of local anisotropy axes (dashed lines) and of ground-state local magnetizations (arrows) on the Dy sites.

magnetization of 12.1 N $\beta$  at 70 kOe (Figure 2 inset) suggest the presence of a significant magnetic anisotropy and/or low-lying excited states.

Both the temperature and frequency dependences of the alternating current (ac) susceptibilities under a zero-dc field (Figures 3 and S3) reveal a slow relaxation of the magnetization that is typical for SMM behavior.  $\chi'$  shows a maximum value which starts to decrease in the 11–23 K range, while  $\chi''$  defines a maximum between 6 (10 Hz) and 19 K (1400 Hz). For most Ln-SMMs, another increase of the ac response is commonly observed in the low-temperature region, which is typical of the onset of pure quantum tunneling.<sup>4a,11c,12</sup> In contrast, both  $\chi'$  and  $\chi''$  components for **1** cascade like avalanches below the blocking temperature and nearly vanish as the temperature approaches 2 K. This signals the “freezing” of the spins by the anisotropy barriers and can be taken as a clear indication of the efficient suppression of zero-field tunneling of magnetization occurring in this complex.

The tunneling pathways were explored on single crystals of **1** using a micro-SQUID technique,<sup>13</sup> with the results shown in Figure 4a,b. Magnetic memory effects, clearly visible below 1.5 K, give rise to a two-step profile hysteresis cycle. It is well known that significant QTM is typically observed in lanthanide-containing single-ion magnets, resulting usually in very small coercive fields.<sup>14</sup> However, in complex **1**, the significantly increasing coercivities with decreasing temperature suggest sluggish quantum tunneling under low-lying states as they progressively depopulate, and this is undoubtedly mediated by the coupling of Dy<sup>III</sup> centers. This conjecture is corroborated by direct measurements of the magnetization relaxation (magnetization decay experiments) performed down to 0.04 K (Figure S4). The quantum regime is observed below 0.15 K, with a characteristic time of  $\tau_{\text{QTM}} = 35$  s (Figure 5). Such a tunneling rate is considerably slow for a dysprosium SMM: 3 orders of magnitude slower than reported for other Dy<sub>2</sub> systems, usually at the millisecond level.<sup>4a,11c,12c,12d,15</sup> QTM has been previously studied for several polynuclear Ln-SMMs with negligible or antiferromagnetic interaction,<sup>4b,15,16</sup> but what makes complex **1** unusual is that it provides an excellent candidate for probing quantum tunneling in a system with ferromagnetically coupled Ln ions.<sup>17</sup>

The nature of the energy states of **1** was revealed by *ab initio* calculations (see Figure S5 and Table S1). The calculated local  $g$  tensors on the dysprosium sites are strongly axial (Table S2). The corresponding local anisotropy axes are almost parallel to each other (inset of Figure 3 and Figure S6), lying approximately in the plane formed by the two dysprosium ions and one bridging oxygen atom

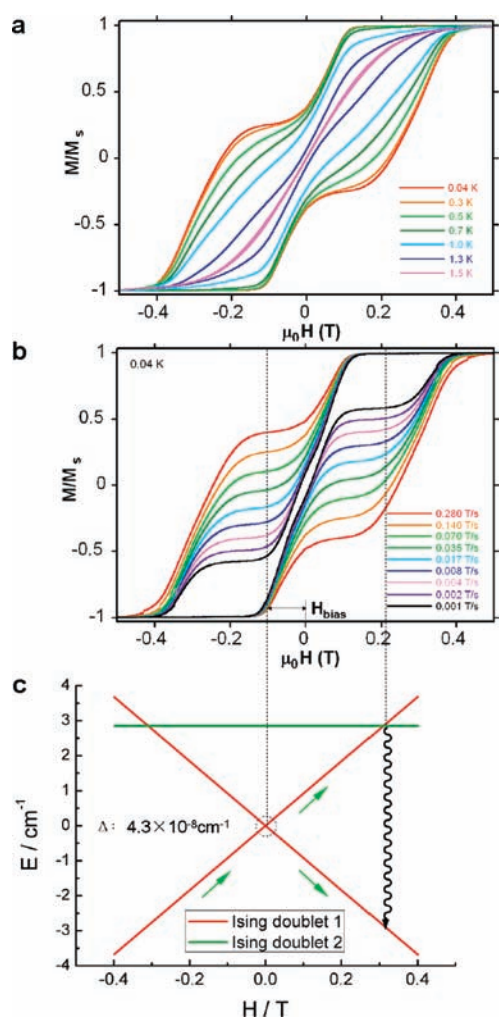


**Figure 4.** Plot of normalized magnetization ( $M/M_s$ ) versus  $\mu_0 H$ . The loops are shown at different temperatures at 0.035 T/s (a) and at different sweep rates at 0.04 K (b). (c) Zeeman diagrams calculated for the field applied along the anisotropy axis of the ground exchange doublet.

(Table S3). Therefore, the transversal components of the dipolar field induced by the dysprosium ions on each other will be small. We can treat the joint effect of the anisotropic dipolar and the exchange interactions ( $J$ ) within the Lines model between the lowest Kramers doublets on the Dy sites<sup>18</sup> and take into account the intermolecular interaction ( $zJ$ ).<sup>19</sup> Figures 2 and S7 show calculated  $\chi_M T$  and  $M(H)$  for a powder for the set  $J = 5.88 \text{ cm}^{-1}$  (each Dy<sup>III</sup> ion is described as  $S = 1/2$ ) and  $zJ = -1.84 \text{ cm}^{-1}$ .

In order to understand the origin of the obtained relatively strong ferromagnetic interaction between the lowest Kramers doublets on the Dy sites, we calculated the dipolar contribution to  $J$ . Using the calculated orientations of local anisotropy axes (Figure 3) and the main values of the local  $g$  tensors (Table S2), we obtain  $J_{\text{dip}} = 5.36 \text{ cm}^{-1}$ . The pure exchange contribution to the interaction is then  $J_{\text{exch}} = J - J_{\text{dip}} = 0.52 \text{ cm}^{-1}$ . Thus, the ferromagnetic coupling comes almost entirely from a ferromagnetic dipolar interaction which, at its turn, originates from a near-parallel alignment of the local anisotropy axes and the line connecting the dysprosium ions.<sup>11a</sup> This is an example of how a strong ferromagnetic interaction between lanthanide ions can be achieved by engineering the local anisotropy axes. We note, however, that this

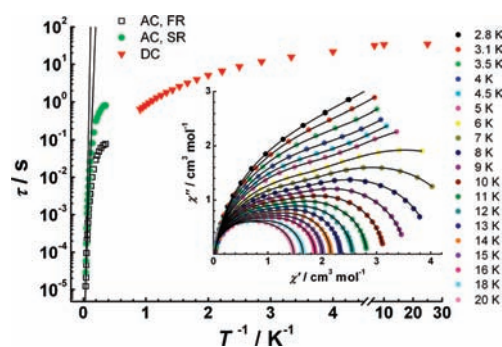


**Figure 5.** Arrhenius plot constructed using ac  $\chi''$  (Table S1) and dc decay data (Figure S4). The dashed lines represent the best fits to the Arrhenius law of the thermally activated region with the parameters given in the text. Inset: Cole–Cole plots for **1**. The solid lines indicate the fits to eq 1.

conclusion is valid for “conventional”, diamagnetic bridges between lanthanide ions, like  $\text{O}_2^{2-}$  from the present case. In the case of lanthanide ions connected by radical bridges, like  $\text{N}_2^{3-}$ , the interaction between them is much stronger,<sup>8</sup> pointing to their preponderant exchange character.

With the obtained parameters  $J$  and  $zJ$ , the spectrum of the lowest exchange multiplets is found to be two exchange Ising doublets (Table S4), separated by  $2.85 \text{ cm}^{-1}$ , each showing a tunneling splitting of the order of  $10^{-8} \text{ cm}^{-1}$  (Figure 4c). The level crossings are responsible for QTM. The shift in magnetization loops (Figure 4b) is attributed to the exchange bias field arising from weak inter-SMM interactions.<sup>19</sup> The negligible tunneling splitting in both exchange doublets points to an almost net Ising exchange interaction between Dy sites. The Ising exchange interaction in such a low-symmetry complex is entirely due to the very low transversal components of the local  $g$  tensors (Table S2) and is the reason for the observed strong suppression of relaxation rate at low temperatures.

In the high-temperature regime, two closely spaced relaxation processes operate, as seen from the broad  $\chi''$  peak (Figures S8 and S9) or significantly broadened Cole–Cole plots (Figure 5 inset). The observation of two relaxations is not unprecedented and is the result of the presence of distinct anisotropic centers.<sup>4b,c,11a</sup> In this specific case, these are uniquely identifiable in this asymmetric dinuclear compound. Despite their proximity, the relaxation time for each process can be extracted by fitting the data to two relaxation processes using the sum of two modified Debye functions:<sup>20</sup>

$$\chi_{ac}(\omega) = \chi_{S,\text{tot}} + \frac{\Delta\chi_1}{1 + (i\omega\tau_1)^{(1-\alpha_1)}} + \frac{\Delta\chi_2}{1 + (i\omega\tau_2)^{(1-\alpha_2)}}, \quad \omega = 2\pi\nu \quad (1)$$

where  $\chi_{S,\text{tot}} = \chi_{S1} + \chi_{S2}$  represents the sum of the adiabatic susceptibilities of the two relaxing species;  $\Delta\chi_i$  is the difference between the adiabatic susceptibility ( $\chi_{Si}$ ) and the isothermal susceptibility ( $\chi_{Ti}$ ) of each magnetic phase. The experimental  $\chi_{ac}(\omega)$  curves between 2.8 and 24 K can be nicely simulated by applying eq 1 and depicted as the  $\chi'(\omega)$ ,  $\chi''(\omega)$ , and Cole–Cole plots in Figure S3 and the inset of Figure 5. The parameters obtained are summarized in Table S5.

Over the temperature range 2.8–24 K, the parameter  $\alpha$ , quantifying the width of the  $\tau$  distribution, was found to be always

less than 0.09. This indicates that each relaxation phase has a very narrow distribution of relaxation times. Plotting the relaxation time versus reciprocal temperature reveals that the Arrhenius-like behavior is linear at very high temperatures, with effective energy barriers of  $U_{\text{eff1}} = 150$  K (pre-exponential factor  $\tau_{01} = 2.3 \times 10^{-8}$  s) and  $U_{\text{eff2}} = 198$  K ( $\tau_{02} = 7.3 \times 10^{-9}$  s) for the fast relaxation (FR) and slow relaxation (SR) phases, respectively (Figures 5 and S10). The *ab initio* calculations revealed that the first excited Kramers doublets on the local dysprosium sites lie much higher in energy (Table S1). This explains why the thermally activated process of the relaxation of magnetization shows up at relatively high temperature (Figure 3). The excitation energies on each local Dy site are larger than the activation barriers derived from the relaxation times; nevertheless, the calculations support the close values of  $U_{\text{eff1}}$  and  $U_{\text{eff2}}$ .

In conclusion, a new alkoxido-bridged asymmetric dinuclear Dy<sup>III</sup> SMM has been assembled using the rigid H<sub>2</sub>ovph ligand. At high temperatures the blockage of magnetization is due to the individual ion anisotropy, which explains the observation of two relaxation times. At low enough temperature the Dy<sub>2</sub> dimer enters the exchange-blocking regime, exhibiting a sluggish relaxation ( $\tau_{\text{QTM}} = 35$  s). The achievement of such long relaxation times  $\tau$  is crucial for information storage applications.<sup>21</sup> The efficient blockage of magnetization in the lowest exchange states of compound **1** is mainly due to the high axiality of the Dy<sup>III</sup> ions, which leads to an Ising type of exchange interaction and, as a result, an almost degenerate lowest exchange doublet (i.e., almost zero intrinsic tunneling gap). The present results demonstrate that, for suitable crystal fields on the Dy sites, strong axiality of the local doublets, leading to an efficient blocking of magnetization, can be achieved also—if not better—in complexes with low symmetry. This provides a promising strategy for enhancing the single-molecule magnet properties of polynuclear lanthanide-based complexes via fine-tuning of the local environments of the lanthanide ions.

## ■ ASSOCIATED CONTENT

**S** Supporting Information. Experimental procedures, physical measurements, crystallography, computational details, Figures S1–S14, and Tables S1–S5. This material is available free of charge via the Internet at <http://pubs.acs.org>.

## ■ AUTHOR INFORMATION

### Corresponding Author

tang@ciac.jl.cn; hongjie@ciac.jl.cn; Liviu.Chibotaru@chem.kuleuven.be

## ■ ACKNOWLEDGMENT

This work was supported by the NSFC of China (20871113, 91022009, and 20921002). Prof. Dr. P. Gamez is gratefully acknowledged for fruitful discussions.

## ■ REFERENCES

- (1) (a) Gatteschi, D.; Sessoli, R.; Villain, J. *Molecular Nanomagnets*; Oxford University Press: Oxford, 2006. (b) Mannini, M.; Pineider, F.; Danieli, C.; Totti, F.; Sorace, L.; Sainctavit, P.; Arrio, M. A.; Otero, E.; Joly, L.; Cezar, J. C.; Cornia, A.; Sessoli, R. *Nature* **2010**, *468*, 417.
- (2) Sessoli, R.; Powell, A. K. *Coord. Chem. Rev.* **2009**, *253*, 2328.
- (3) (a) AlDamen, M. A.; Clemente-Juan, J. M.; Coronado, E.; Martí-Gastaldo, C.; Gaita-Arino, A. *J. Am. Chem. Soc.* **2008**, *130*, 8874. (b) Ishikawa, N.; Sugita, M.; Ishikawa, T.; Koshihara, S.-y.; Kaizu, Y. *J. Am. Chem. Soc.* **2003**, *125*, 8694.

- (4) (a) Lin, P. H.; Burchell, T. J.; Clérac, R.; Murugesu, M. *Angew. Chem., Int. Ed.* **2008**, *47*, 8848. (b) Lin, P. H.; Burchell, T. J.; Ungur, L.; Chibotaru, L. F.; Wernsdorfer, W.; Murugesu, M. *Angew. Chem., Int. Ed.* **2009**, *48*, 9489. (c) Guo, Y.-N.; Xu, G.-F.; Gamez, P.; Zhao, L.; Lin, S.-Y.; Deng, R.; Tang, J.; Zhang, H.-J. *J. Am. Chem. Soc.* **2010**, *132*, 8538. (d) Hewitt, I. J.; Tang, J.; Madhu, N. T.; Anson, C. E.; Lan, Y.; Luzon, J.; Etienne, M.; Sessoli, R.; Powell, A. K. *Angew. Chem., Int. Ed.* **2010**, *49*, 6352.
- (5) Rinehart, J. D.; Meihaus, K. R.; Long, J. R. *J. Am. Chem. Soc.* **2010**, *132*, 7572.
- (6) Wang, Y.; Li, X.-L.; Wang, T.-W.; Song, Y.; You, X.-Z. *Inorg. Chem.* **2009**, *49*, 969.
- (7) (a) Luis, F.; Martínez-Pérez, M. J.; Montero, O.; Coronado, E.; Cardona-Serra, S.; Martí-Gastaldo, C.; Clemente-Juan, J. M.; Sesé, J.; Drung, D.; Schurig, T. *Phys. Rev. B* **2010**, *82*, 060403. (b) Giraud, R.; Wernsdorfer, W.; Tkachuk, A. M.; Maily, D.; Barbara, B. *Phys. Rev. Lett.* **2001**, *87*, 057203. (c) Wernsdorfer, W.; Ohm, T.; Sangregorio, C.; Sessoli, R.; Maily, D.; Paulsen, C. *Phys. Rev. Lett.* **1999**, *82*, 3903. (d) Ishikawa, N.; Sugita, M.; Wernsdorfer, W. *J. Am. Chem. Soc.* **2005**, *127*, 3650. (e) Ishikawa, N.; Sugita, M.; Wernsdorfer, W. *Angew. Chem., Int. Ed.* **2005**, *44*, 2931.
- (8) Rinehart, J. D.; Fang, M.; Evans, W. J.; Long, J. R. *Nat. Chem.* **2011**, *3*, 538.
- (9) (a) Runschke, C.; Meyer, G. Z. *Anorg. Allg. Chem.* **1997**, *623*, 1493. (b) Ruiz-Martinez, A.; Casanova, D.; Alvarez, S. *Chem.—Eur. J.* **2008**, *14*, 1291.
- (10) Kahn, M. L.; Ballou, R.; Porcher, P.; Kahndagger, O.; Sutter, J.-P. *Chem.—Eur. J.* **2002**, *8*, 525.
- (11) (a) Hewitt, I. J.; Lan, Y.; Anson, C. E.; Luzon, J.; Sessoli, R.; Powell, A. K. *Chem. Commun.* **2009**, 6765. (b) Hussain, B.; Savard, D.; Burchell, T. J.; Wernsdorfer, W.; Murugesu, M. *Chem. Commun.* **2009**, 1100. (c) Xu, G. F.; Wang, Q. L.; Gamez, P.; Ma, Y.; Clérac, R.; Tang, J. K.; Yan, S. P.; Cheng, P.; Liao, D. Z. *Chem. Commun.* **2010**, 46, 1506.
- (12) (a) Ishikawa, N.; Sugita, M.; Tanaka, N.; Ishikawa, T.; Koshihara, S.-y.; Kaizu, Y. *Inorg. Chem.* **2004**, *43*, 5498. (b) AlDamen, M. A.; Cardona-Serra, S.; Clemente-Juan, J. M.; Coronado, E.; Gaita-Arino, A.; Martí-Gastaldo, C.; Luis, F.; Montero, O. *Inorg. Chem.* **2009**, *48*, 3467. (c) Ma, Y.; Xu, G.-F.; Yang, X.; Li, L.-C.; Tang, J.; Yan, S.-P.; Cheng, P.; Liao, D.-Z. *Chem. Commun.* **2010**, 8264. (d) Layfield, R. A.; McDouall, J. J. W.; Sulway, S. A.; Tuna, F.; Collison, D.; Winpenny, R. E. P. *Chem.—Eur. J.* **2010**, *16*, 4442. (e) Bernot, K.; Pointillart, F.; Rosa, P.; Etienne, M.; Sessoli, R.; Gatteschi, D. *Chem. Commun.* **2010**, 46, 6458.
- (13) Wernsdorfer, W. *Adv. Chem. Phys.* **2001**, *118*, 99.
- (14) (a) Jiang, S.-D.; Wang, B.-W.; Sun, H.-L.; Wang, Z.-M.; Gao, S. J. *Am. Chem. Soc.* **2011**, *133*, 4730. (b) Habib, F.; Lin, P.-H.; Long, J.; Korobkov, I.; Wernsdorfer, W.; Murugesu, M. *J. Am. Chem. Soc.* **2011**, *133*, 8830.
- (15) Long, J.; Habib, F.; Lin, P.-H.; Korobkov, I.; Enright, G.; Ungur, L.; Wernsdorfer, W.; Chibotaru, L. F.; Murugesu, M. *J. Am. Chem. Soc.* **2011**, *133*, 5319.
- (16) Lin, P.-H.; Korobkov, I.; Wernsdorfer, W.; Ungur, L.; Chibotaru, L. F.; Murugesu, M. *Eur. J. Inorg. Chem.* **2011**, 1535.
- (17) Katoh, K.; Kajiwara, T.; Nakano, M.; Nakazawa, Y.; Wernsdorfer, W.; Ishikawa, N.; Breedlove, B. K.; Yamashita, M. *Chem.—Eur. J.* **2011**, *17*, 117.
- (18) (a) Chibotaru, L. F.; Ungur, L.; Aronica, C.; Elmoll, H.; Pilet, G.; Luneau, D. *J. Am. Chem. Soc.* **2008**, *130*, 12445. (b) Ungur, L.; Heuvel, W. V. d.; Chibotaru, L. F. *New J. Chem.* **2009**, *33*, 1224.
- (19) (a) Lecren, L.; Wernsdorfer, W.; Li, Y. G.; Roubeau, O.; Miyasaka, H.; Clérac, R. *J. Am. Chem. Soc.* **2005**, *127*, 11311. (b) Yang, E. C.; Harden, N.; Wernsdorfer, W.; Zakharov, L.; Brechin, E. K.; Rheingold, A. L.; Christou, G.; Hendrickson, D. N. *Polyhedron* **2003**, *22*, 1857. (c) Tasiopoulos, A. J.; Wernsdorfer, W.; Moulton, B.; Zaworotko, M. J.; Christou, G. *J. Am. Chem. Soc.* **2003**, *125*, 15274.
- (20) Grah, M.; Kotzler, J.; Sessler, I. *J. Magn. Magn. Mater.* **1990**, *90–1*, 187.
- (21) Aronica, C.; Pilet, G.; Chastanet, G.; Wernsdorfer, W.; Jacquot, J. F.; Luneau, D. *Angew. Chem., Int. Ed.* **2006**, *45*, 4659.